

# Optimizing tensile strength at MAG welding process of S235JR steel

**Sabi Sabev**

Technical University of Sofia,  
Branch Plovdiv  
Plovdiv, Bulgaria  
sabi\_sabev@tu-plovdiv.bg

**Konstantin Chukalov**

Technical University of Sofia,  
Branch Plovdiv  
Plovdiv, Bulgaria  
chukalov@tu-plovdiv.bg

**Abstract.** The article is of an experimental nature for welding S235JR by MAG welding method. The purpose of this work is to optimize the welding parameters of MAG welding using shield two-component gas argon 18 to achieve ultimate tensile strength. The experiment is according to central composition design and 13 experiments were made. Samples with dimensions of 100x40x4 mm were tested with a universal tension-compression machine. Statistical processing was done and a regression relationship between welding current and seam width on the maximum tensile strength was obtained.

**Keywords:** MAG welding process, tensile strength, optimization methods, regression analyze, central composition design, S235JR.

## I. INTRODUCTION

Low carbon steel S235JR is widely used in mechanical engineering [1]. It is characterized by good plasticity, low hardness, low tensile strength, good weldability [2]. It is processed most often by cutting, forging and welding. It is used for structural details such as rivets, chains, bolts, etc.

MAG welding is characterized by a number of advantages - no pores, high precision, smooth welds[3],[4]. With MAG welding, high current loads are achieved on the electrode, which leads to concentrated heating with a large penetration depth, high speed and high productivity. The MAG method is preferred for welding of carbon steels, as well as low and medium alloyed steels.

CORGON 18 is a two-component mixture comprising 82% argon and 18% carbon dioxide. This gas shield is selected because it leads to good penetration and sidewall fusion.

One of the main welding modes is the current, which at high values in MAG welding leads to a deep penetration and higher productivity, but with too high current leads to undercuts and low quality of welding[5]. The relation of the welding current and the width of the seam on the tensile

strength of a welded parts made of low carbon steel S235JR was experimentally investigated[6]

## General Regulations

The structural steel used in the experiment was S235JR[7]. Samples with dimensions of 100x40x4 mm were used. MAG welding method and two-component shielding weld, CORGON 18: 82% Ar + 18% CO<sub>2</sub>, were used. The filler material is SG2 TYSWELD with a diameter of 0.8 mm solid copper wire for MIG/MAG welding of carbon and low-alloyed steels.

Welding was done with a SHERMAN DIGIMIG 200 PULSE welding machine. with the following parameters: Wire feeding speed 2 – 14 m/min ,welding current range 24-200A Welding voltage 17.5-24.7V Works with welding wire D200/5kg (0.6-0.8mm) [8].

The following design of the experiment was made, using the central composite design [9],[10]. This plan contains a built-in factorial or fractional factorial plan with center points, which is supplemented with a group of "star points" that allow curvature estimation[11]. If the distance from the center of the design space to the factor point  $\pm 1$  for each factor, the distance from the center of the design space to the star point is  $|\alpha|=1.41$ , as shown in Fig.1.



Fig. 1. Sherman digimig 200 pulse.

Print ISSN 1691-5402

Online ISSN 2256-070X

<https://doi.org/10.17770/etr2024vol3.8140>

© 2024 Sabi Sabev, Konstantin Chukalov. Published by Rezekne Academy of Technologies.  
This is an open access article under the [Creative Commons Attribution 4.0 International License](https://creativecommons.org/licenses/by/4.0/).

The resulting design of the experiment was made using Minitab, tab. 1. The value of  $\alpha$  in this two-factor design was 1.41 and a total of 13 trials were obtained, with 5 trials selected at the center of the cube. The minimum and maximum values of the controlled factors are as follows:

- Welding current I – range 50A-180A
- Welding width b – range - 0mm-6mm

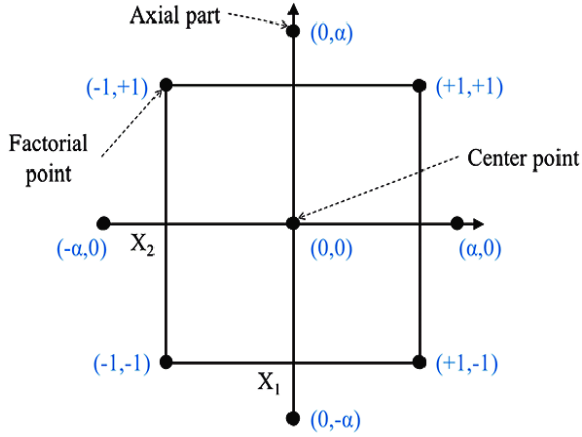


Fig. 2. The central compositional design.

TABLE 1 THE PLAN OF THE EXPERIMENT

| Run | I     | $\delta$ | I   | $\delta$ |
|-----|-------|----------|-----|----------|
| 1   | -1,00 | 1,00     | 69  | 5,1      |
| 2   | -1,00 | -1,00    | 69  | 0,9      |
| 3   | -1,41 | 0,00     | 50  | 3,0      |
| 4   | 1,41  | 0,00     | 180 | 3,0      |
| 5   | 0,00  | 1,41     | 115 | 6,0      |
| 6   | 0,00  | 0,00     | 115 | 3,0      |
| 7   | 0,00  | 0,00     | 115 | 3,0      |
| 8   | 0,00  | 0,00     | 115 | 3,0      |
| 9   | 0,00  | 0,00     | 115 | 3,0      |
| 10  | 1,00  | 1,00     | 161 | 5,1      |
| 11  | 0,00  | -1,41    | 115 | 0,0      |
| 12  | 1,00  | -1,00    | 161 | 0,9      |
| 13  | 0,00  | 0,00     | 115 | 3,0      |

The specimens are tested using a universal tensile compression testing machine[12]. The test set-up is shown in Fig.2.



Fig. 3. Testing set-up.

On the samples, after welding, manual mechanical processing of the welding seam was done, fig.3.

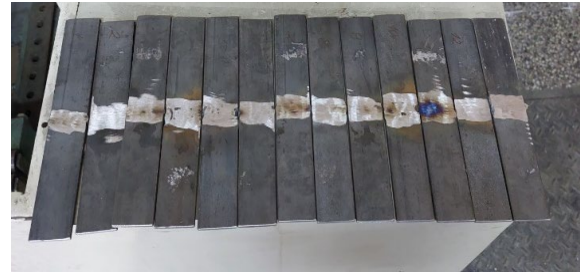


Fig. 4. Samples after manual mechanical processing.

## II. RESULTS AND DISCUSSION

During the experiment, the test body is fixed in the jaws of the machine, then the motor is turned on and one jaw is driven, increasing the load until the specimen is ruptured-fig5.



Fig. 5. Destruction of samples and checking the values.

After conducting the experiment, the results at different current sizes and seam widths and the obtained maximum tensile strength are presented in tabular form tab.2.

TABLE 2.EXPERIMENTAL RESULTS

| No | I [A]  | b [mm] | F [t] | Rm [Pa]  |
|----|--------|--------|-------|----------|
| 1  | 69,04  | 5,12   | 6,65  | 4,08E+08 |
| 2  | 69,04  | 0,88   | 3,25  | 1,99E+08 |
| 3  | 50,00  | 3,00   | 4,40  | 2,70E+08 |
| 4  | 180,00 | 3,00   | 6,15  | 3,77E+08 |
| 5  | 115,00 | 6,00   | 8,15  | 5,00E+08 |
| 6  | 115,00 | 3,00   | 6,30  | 3,86E+08 |
| 7  | 115,00 | 3,00   | 6,50  | 3,98E+08 |
| 8  | 115,00 | 3,00   | 7,65  | 4,69E+08 |
| 9  | 115,00 | 3,00   | 6,75  | 4,14E+08 |
| 10 | 160,96 | 5,12   | 6,80  | 4,17E+08 |
| 11 | 115,00 | 0,00   | 3,55  | 2,18E+08 |
| 12 | 160,96 | 0,88   | 3,75  | 2,30E+08 |
| 13 | 115,00 | 3,00   | 7,15  | 4,38E+08 |

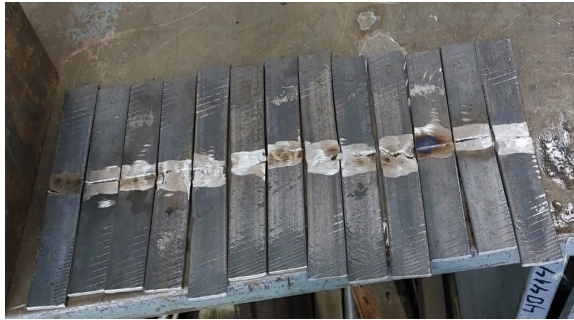


Fig. 6. Samples after testing.

Mathematical and statistical processing was performed with the program product MINITAB[14]. The data from Table 2 were processed and the following regression model was obtained [15]:

$$F = -3.36 + 1.601 b + 0.1078 I - 0.1390 b * b - 0.000432 I * I \quad (1)$$

Where

b-welding width

I – welding current

The coefficient of determination is  $R^2 = 93.58\%$ , and the corrected coefficient of determination-  $R_{adj}^2 = 90.38\%$ , tab. 3.

TABLE 3 PARAMETERS OF THE MODEL

| S   | R-sq   | R-sq(adj) | PRESS  | R-sq(pred) | AICc | BIC  |
|-----|--------|-----------|--------|------------|------|------|
| 0.5 | 93.58% | 90.38%    | 6.0682 | 81.03%     | 38.9 | 28.3 |

From the condition for the  $R^2$ -coefficient of multiple correlation, which is defined as insignificant. From the analysis of the variables, shown in table 4, it may be seen that the P value of the coefficient I is above 0.05 and is insignificant.

TABLE 4 COEFFICIENTS OF THE MODEL

| Source     | DF | Seq SS  | Contribution | Adj SS | Seq MS  | F-Value | P-Value |
|------------|----|---------|--------------|--------|---------|---------|---------|
| Regression | 4  | 29,9404 | 93,58%       | 29,94  | 7,4851  | 29,17   | 0       |
| b          | 1  | 21,1425 | 66,08%       | 9,0411 | 21,1425 | 82,4    | 0       |
| I          | 1  | 1,1819  | 3,69%        | 6,5884 | 1,1819  | 4,61    | 0,064   |
| b*b        | 1  | 1,8157  | 5,68%        | 2,7228 | 1,8157  | 7,08    | 0,029   |
| I*I        | 1  | 5,8003  | 18,13%       | 5,8003 | 5,8003  | 22,61   | 0,001   |
| Error      | 8  | 2,0527  | 6,42%        | 2,0527 | 0,2566  |         |         |
| Lack-of-   | 4  | 0,8897  | 2,78%        | 0,8897 | 0,2224  | 0,77    | 0,599   |
| Pure Error | 4  | 1,163   | 3,64%        | 1,163  | 0,2908  |         |         |

The Pareto diagram, Fig. 7 shows the absolute values of the standardized effects from the most important to unimportant ones [16]. The chart also draws a reference line which effects are statistically significant. It may be seen that component B is behind the significance line, therefore the coefficient is insignificant.

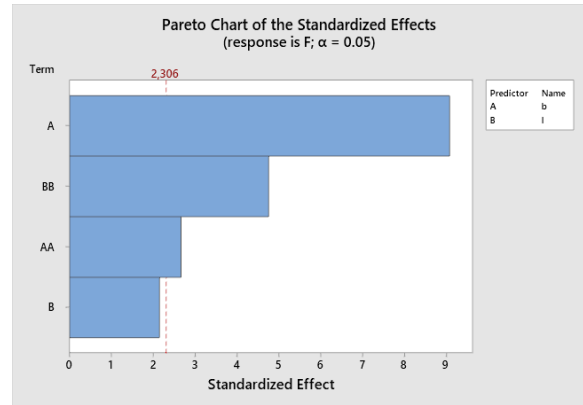


Fig. 7. Pareto diagram.

Analysis of residuals is performed using the standardized residuals plots in Fig. 8.[17]. The values of the standardized residuals should be within  $\pm 2$ . Values close to 2 are sample No4 and No8. Also on the same samples, pores from welding process are observed fig.9. These results are removed and the process was repeated.

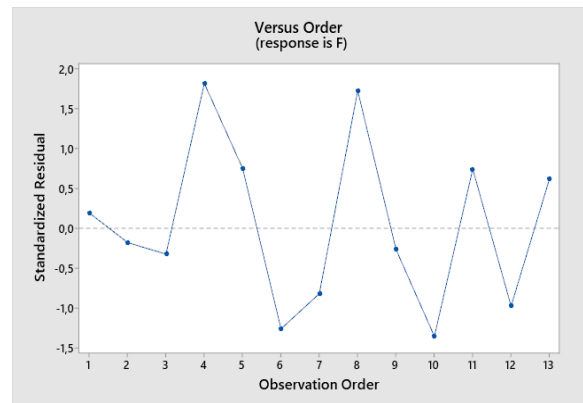


Fig. 8. Standardized residuals.



Fig. 9. Pores in samples No4 and No8.

After the operation the following results are obtained.

$$F = -3.658 + 1.345 b + 0.1220 I - 0.0965 b * b - 0.000519 I * I \quad (2)$$

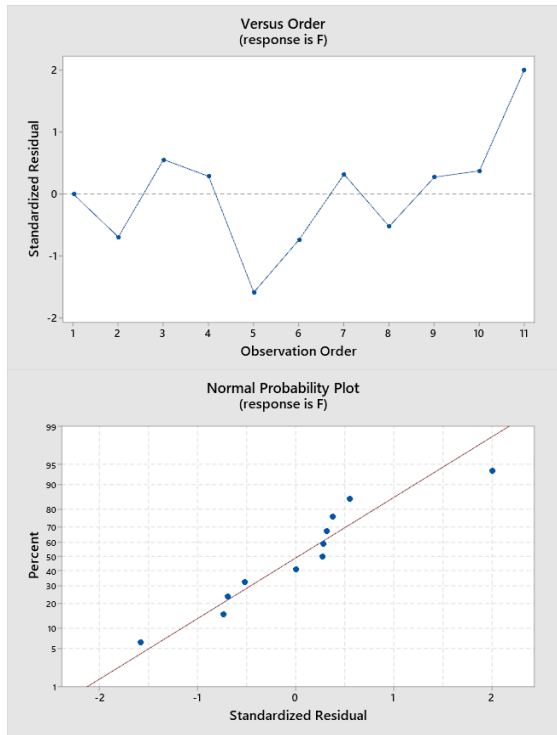


Fig. 10. Standardized residuals.

The new coefficient of determination was calculated  $R^2 = 98.43\%$ , and the corrected coefficient is  $R^2_{adj} = 97.39\%$  tab. 5 and tab. 6.

TABLE 5 PARAMETERS OF THE MODEL

| S     | R-sq   | R-sq(adj) | PRESS    | R-sq(pred) | AICc | BIC   |
|-------|--------|-----------|----------|------------|------|-------|
| 0,273 | 98,43% | 97,39%    | 0,957393 | 96,65%     | 29   | 10,39 |

F - Value of the Fisher distribution used to test significance of the multiple correlation coefficient.

$R^2$  - Multiple correlation coefficient is significant.

From the analysed variables, shown in Table 6, all the P values are below 0.05 so are significant.

The analysis of standardized residuals fig. 10, shows that there are no critical errors.

TABLE 6 COEFFICIENTS OF THE MODEL

| Source      | DF | Seq SS  | Contribution | Adj SS  | Seq MS  | F-Value | P-Value |
|-------------|----|---------|--------------|---------|---------|---------|---------|
| Regression  | 4  | 28,1644 | 98,43%       | 28,1644 | 7,0411  | 94,32   | 0       |
| b           | 1  | 21,1425 | 73,89%       | 5,5861  | 21,1425 | 283,22  | 0       |
| I           | 1  | 1,0766  | 3,76%        | 5,633   | 1,0766  | 14,42   | 0,009   |
| b*I         | 1  | 1,1319  | 3,96%        | 1,1319  | 1,1319  | 15,16   | 0,008   |
| I*I         | 1  | 4,8133  | 16,82%       | 4,8133  | 4,8133  | 64,48   | 0       |
| Error       | 6  | 0,4479  | 1,57%        | 0,4479  | 0,0747  |         |         |
| Lack-of-Fit | 3  | 0,0454  | 0,16%        | 0,0454  | 0,0151  | 0,11    | 0,947   |
| Pure Error  | 3  | 0,4025  | 1,41%        | 0,4025  | 0,1342  |         |         |

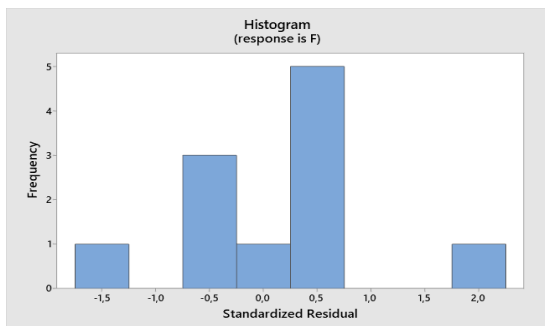


Fig. 11. Histogram of standardized residuals.

The Pareto diagram, fig.12 shows that the components are in front of the significance line [18].

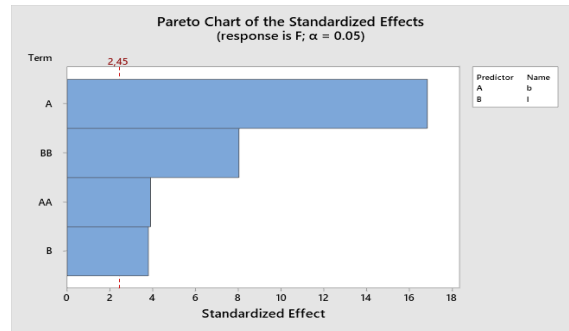


Fig. 12. Pareto diagram.

The influence of welding current and width of the seams on the tensile strength is also analyzed, fig. 13.

The one-parameter optimization was processed with MINITAB software, with the help of which the maximum values for the objective function - tensile strength - were found. The data are presented in Fig.14. The maximum value of tensile strength is under the following conditions: width of the seam - 6mm and magnitude of the current is 117A.

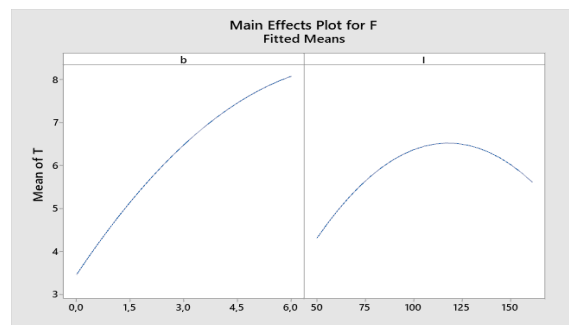


Fig. 13. Influence of the components.

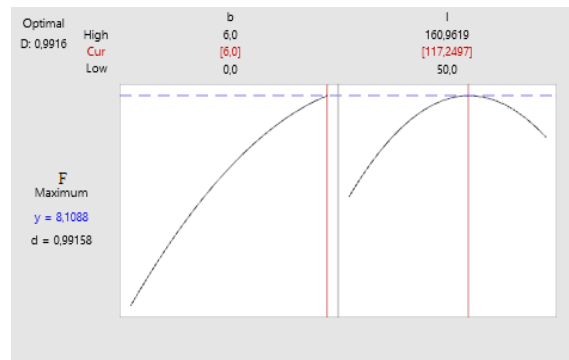


Fig. 14. Optimization diagram.

### III. CONCLUSIONS

By experimental planning the number of trials was reduced to 13- enough to statistical processing. For the goals of the article are selected 2 welding parameters that have influence on technological parameters of welding parts. Tensile strength is selected for output parameter because shows entire engineering performance of selected material.

The following conclusions drawn from the experimental results and their processing:

1. An adequate regression model was designed describing the relationship between welding current, and tensile strength.

2. Two errors caused by pores during welding were established.

3. From the regression analysis, the welding current factor affects the least, and the distance  $b$  affects about 78% on the tensile strength objective function.

4. From fig.13 it is also seen that the greatest influence on the maximum tensile strength is exerted by the width of the seam in this research.

5. One-parameter optimization of tensile strength was done.

Similar optimizations articles of MAG welding parameters prove credibility and the actuality of the method and the experimental results [19], [20], [21].

#### IV. ACKNOWLEDGMENTS

The authors would like to thank the Research and Development Sector at the Technical University of Sofia for the financial support.

#### REFERENCES

- [1] S. Yuan, H. Xie, H. Wu, M. Ren, X. Liang, S. Jiao, Z. Jiang The Effects of Annealing on Microstructure and Mechanical Properties of Monolithic Low Carbon Steel and Medium Manganese Steel/low Carbon Steel (Mn8/SS400) Bimetal Composite, Proceedings of the 14th International Conference on the Technology of Plasticity - Current Trends in the Technology of Plasticity, 2023 [https://doi.org/10.1007/978-3-031-41341-4\\_73](https://doi.org/10.1007/978-3-031-41341-4_73)
- [2] V. F. Khorunov, I. Zvolinsky, S. Maksymova, ARC BRAZING OF LOW-CARBON STEELS, 2023
- [3] C. Gonzales, H. Ortega, E. Garcia, J. Cabello, Environmental and Economic Analyses of TIG, MIG, MAG and SMAW Welding Processes, Metals 13(6):1094, 2023 <https://doi.org/10.3390/met13061094>
- [4] Y. Cho, B. Kim, C. Lee, N. Kang, Mechanical properties of one-sided welding for the low-temperature steel using a high-current MAG welding, Welding in the World, Le Soudage D, 2023 <https://doi.org/10.1007/s40194-023-01585-5>
- [5] D. Salvador, Welding Certification and Standards: Ensuring Quality and Reliability in Fabrication, International Journal of Advanced Research in Science Communication, 2023 <http://dx.doi.org/10.48175/IJAR SCT-11905>
- [6] H. Zhang, R. Li, S. Yang, L. Zhan, M. Xiong, B. Wang, J. Jhang, Experimental and Simulation Study on Welding Characteristics and Parameters of Gas Metal Arc Welding for Q345qD Thick-Plate Steel, Materials 16(17):5944, 2023 <https://doi.org/10.3390/ma16175944>
- [7] W. Kraus, H. Blum, Structural Steel Fabrication with Mixed Reality, ce/papers 6(3-4):904-907, 2023 <https://doi.org/10.1002/cepa.2575>
- [8] S. Tsumura, E. Meirelles, V. Callil, M. Lourenco, J. Caprepe, Parametric Analysis of Welding Parameters for Hybrid Laser/MAG Welding, 11th International Seminar on Inland Waterways and Waterborne Transportation, 2019 <https://doi.org/10.3390/ma15124328>
- [9] M. Tabat, M. Kibria, E. Epele, S. McCoy, Optimization for Sustainable Process Design, 2023 Annual AIChE Meeting (161 - Advances in Process Design I), 2023
- [10] T. Reddy, G. Henze, Optimization Methods, Applied Data Analysis and Modeling for Energy Engineers and Scientists, 2023 <https://doi.org/10.1007/978-1-4419-9613-8>
- [11] A. Hagelberg, D. Andre, M. Finnis, Laboratory multistatic and multipolar SAR CCD investigation, 5th International Conference on Synthetic Aperture in Sonar and Radar At: Lercini, Italy, 2023
- [12] A. Ghazai, The Process of Maintenance and Assessment of The Universal Testing Material Machine H50KS, 2023 <https://doi.org/10.17303/jmsa.2020.4.204>
- [13] S. Pop, M. Dudescu, L. Contac, R. Pop, Evaluation of the tensile properties of polished and unpolished 3D SLA- and DLP-Printed specimens used for surgical guides fabrication, 2023 <http://dx.doi.org/10.2478/asmj-2023-0003>
- [14] M. Evans, C. St, MINITAB Manual, 2023
- [15] B. Hirsh, Regression Analysis, 2022
- [16] S. Kone, N. Kaufmann, L. Richert, Adaptive Algorithms for Relaxed Pareto Set Identification, 2023 <https://doi.org/10.48550/arXiv.2307.00424>
- [17] P. Araripe, I. Lara Ordinal data and residual analysis: Review and application, Brazilian Journal of Biometrics 41(3):287-310, 2023 <http://dx.doi.org/10.28951/bjb.v41i3.637>
- [18] H. Maurer, C. Kaya, Optimization over the Pareto front of nonconvex multi-objective optimal control problems, Computational Optimization and Application, 2023 <https://doi.org/10.1007/s10589-023-00535-7>
- [19] S. Apay, Optimization of Welding Parameters in MAG Lap Welding of DD13 Sheet Metal with Taguchi Method and FEM Analysis, 2022
- [20] H. Wu, Z. Zhang, W. Qi, R. Tian, C. Shi, Optimization of narrow groove plasma-MAG hybrid welding process parameters, 2017
- [21] Z. Li, Y. Xia, Heat source modeling, penetration analysis and parametric optimization of super spray MAG welding, Scientific reports, 2023 <http://dx.doi.org/10.1038/s41598-023-36505-6>